Published in final edited form as:
Cell. 2014 September 11; 158(6): 1348–1361. doi:10.1016/j.cell.2014.07.049.

Antagonistic Control of Social Behaviors by Inhibitory and Excitatory Neurons in the Medial Amygdala

Weizhe Hong[1], **Dong-Wook Kim**[2], and **David J. Anderson**[1,*]

[1]Division of Biology and Biological Engineering, Howard Hughes Medical Institute, California Institute of Technology, Pasadena, CA 91125, USA

[2]Program of Computation and Neural Systems, California Institute of Technology, Pasadena, CA 91125, USA

SUMMARY

Animals display a range of innate social behaviors that play essential roles in survival and reproduction. While the medial amygdala (MeA) has been implicated in prototypic social behaviors such as aggression, the circuit-level mechanisms controlling such behaviors are not well understood. Using cell-type specific functional manipulations, we find that distinct neuronal populations in the MeA control different social and asocial behaviors. A GABAergic subpopulation promotes aggression and two other social behaviors, while neighboring glutamatergic neurons promote repetitive self-grooming, an asocial behavior. Moreover, this glutamatergic subpopulation inhibits social interactions independently of its effect to promote self-grooming, while the GABAergic subpopulation inhibits self-grooming, even in a non-social context. These data suggest that social vs. repetitive asocial behaviors are controlled in an antagonistic manner by inhibitory vs. excitatory amygdala subpopulations, respectively. These findings provide a framework for understanding circuit-level mechanisms underlying opponency between innate behaviors, with implications for their perturbation in psychiatric disorders.

INTRODUCTION

Animals exhibit a broad range of innate behaviors that are essential for their survival and reproduction. These include responses to predators or prey, social behaviors among conspecifics, as well as solitary behaviors such as self-grooming (Tinbergen, 1951). The control of innate social behaviors, while observed throughout the animal kingdom, is of

*Correspondence: wuwei@caltech.edu.

SUPPLEMENTAL INFORMATION
Supplemental information includes Extended Experimental Procedures and seven figures.

AUTHOR CONTRIBUTIONS
W.H. and D.J.A. designed and W.H. performed most of the experiments. D.-W.K. performed electrophysiological recordings. D.J.A supervised the project. W.H. and D.J.A wrote the manuscript.

particular importance in social species such as humans (Stanley and Adolphs, 2013). Abnormalities in social behaviors are associated with several psychiatric disorders (Couture et al., 2010; Sasson et al., 2007).

An important brain region implicated in the control of innate social behaviors is the medial amygdala (MeA) (Kondo, 1992; Kondo and Arai, 1995; Lehman et al., 1980; Newman, 1999). The MeA is one of over a dozen subdivisions of the amygdala (Pitkänen et al., 1997; Swanson and Petrovich, 1998), and is anatomically distinct from amygdala nuclei involved in conditioned fear (Duvarci and Pare, 2014; Ehrlich et al., 2009; Paré et al., 2004). It is located only two synapses away from the vomeronasal organ (VNO), a sensory epithelium that detects pheromonal signals (Dulac and Torello, 2003; Zufall and Leinders-Zufall, 2007), and projects to hypothalamic regions involved in social and other motivated behaviors (Swanson, 2000). Thus, the MeA is situated at an early stage in sensory information processing, suggesting that it may function at a relatively high level in behavioral decision hierarchies (Tinbergen, 1951).

MeA neurons are active during social behaviors such as fighting and mating, and in response to chemosensory cues, as evidenced by induction of c-fos, a surrogate marker of neuronal activity (Choi et al., 2005; Erskine, 1993; Kollack and Newman, 1992; Kollack-Walker and Newman, 1995; Veening et al., 2005), as well as by electrophysiology (Bergan et al., 2014; Bian et al., 2007). Although lesion studies have implicated the MeA in male mating (Kondo, 1992; Kondo and Arai, 1995; Lehman et al., 1980), in the case of aggression the direction of its influence is not clear: in some studies MeA lesions decreased aggression (Kemble et al., 1984; Takahashi and Gladstone, 1988; Wang et al., 2013), while in others they increased it, or had no effect (Busch and Barfield, 1974; Rosvold et al., 1954; Vochteloo and Koolhaas, 1987).

The conclusion that the MeA plays a role in social behavior leaves open the question of how it performs this function. On the one hand, the MeA may control social behaviors in a positive-acting manner. In the simplest version of this hypothesis, activation of MeA neurons in response to chemosensory cues would promote social behavior, while in the absence of such activity social behavior would not occur (Figure S1A). However, the MeA is known to contain heterogeneous neuronal subpopulations (Bian et al., 2007; Choi et al., 2005; Niimi et al., 2012; Xu et al., 2012), whose functions in social behavior are unknown. This raises the possibility that the MeA may control social behaviors in a more complex manner that involves distinct cell types, which may have different or even opponent roles (Figure S1B).

Here we have investigated the cellular control of social behavior by performing functional manipulations of distinct neuronal subpopulations within the posterior dorsal subdivision of MeA (MeApd) (Canteras et al., 1995; Dong et al., 2001; Swanson, 2000). Our experiments reveal that GABAergic neurons in MeApd promote aggression as well as two other innate social behaviors, mating and social grooming. In contrast, neighboring but non-overlapping glutamatergic neurons in MeApd (and adjacent LHA) promote repetitive self-grooming, an asocial behavior. Moreover, the glutamatergic neurons inhibit social behaviors, in a manner independent of their effect to promote self-grooming. Conversely, GABAergic MeApd

neurons suppress self-grooming, in both social and non-social contexts. Thus, the MeApd controls both social and repetitive asocial behaviors, via non-overlapping subpopulations of inhibitory and excitatory neurons, respectively, each of which exerts both positive-acting and antagonistic, negative-acting influences.

RESULTS

Functional identification of MeApd in aggressive behavior

The MeApd has been implicated in social behaviors (Newman, 1999; Swanson, 2000). As a first step towards dissecting the function of MeApd, we focused on offensive inter-male aggression between conspecifics, a prototypic social behavior (Adams, 2006; Blanchard et al., 2003; Kruk, 1991; Siegel et al., 1999). c-fos induction studies have shown that the MeApd is activated during offensive aggression (Lin et al., 2011; Nelson and Trainor, 2007; Newman, 1999; Veening et al., 2005). We confirmed that MeApd exhibits elevated expression of c-fos in resident males that had recently attacked an intruder (Figures 1A–1D). To determine whether c-fos expression is associated with attack, or simply with exposure to conspecific sensory cues, we compared its induction during aggression vs. social investigations that did not lead to attack (Figures 1B–1C). Social investigation in the latter cases occupied ~40% of the total observation period, and was associated with a ~3-fold increase in c-fos expression. However the level of c-fos expression in MeApd following episodes of attack was much higher (Figures 1B–D). Thus MeApd is active during both social investigation and attack, but more strongly so during the latter, consistent with our recent observations in the ventrolateral subdivision of the ventromedial hypothalamus (VMHvl) (Lee et al., 2014).

Although lesion studies have suggested that MeApd is involved in aggression, the evidence regarding the valence of its influence is contradictory. Therefore, it was not clear whether activation of MeApd neurons would promote or inhibit attack. Moreover, while MeApd is activated by pheromonal signals (Chamero et al., 2007; Kollack-Walker and Newman, 1995; Veening et al., 2005), attack requires chemosensory input from the main as well as the accessory olfactory systems (Dhungel et al., 2011; Mandiyan et al., 2005; Stowers et al., 2002; Yoon et al., 2005). This raises the question of where in this circuitry such convergent sensory input is transformed into a coherent program of aggressive behavior. On the one hand, this transformation might occur in structures downstream of MeApd, such as VMHvl (Lee et al., 2014; Lin et al., 2011; Yang et al., 2013); on the other hand, MeApd itself might be sufficient to evoke attack.

To distinguish between these alternatives, we injected wild type C57BL/6N male mice with a mixture of AAV viruses encoding Cre (CMV-Cre) and a Cre-dependent channelrhodopsin 2 (ChR2) (Boyden et al., 2005) (Figures 1E, S2A). The ChR2 virus (AAV-EF1α-FLEX-ChR2-2A-hrGFP) contained a nuclear hrGFP reporter (Lee et al., 2014), allowing visualization of ChR2-expressing cell bodies (Figures 1E, S2A). Successful photostimulation of MeApd neurons *in vivo* via an implanted optic fiber (Aravanis et al., 2007) was confirmed by double labeling for hrGFP and c-fos (Figures 1F–1G).

We examined next the behavioral effects of optogenetic stimulation of MeApd neurons in resident mice in their home cage under infrared light, using the resident-intruder assay (Blanchard et al., 2003). We focused our studies on offensive aggression, a form of aggression that consists of biting and tussling and is initiated by resident animals (see Methods). To avoid any intruder-initiated aggression, a more submissive mouse was used as the intruder (see Methods). The sessions were video recorded in a customized chamber with two synchronized infrared video cameras at a 90° angle (Figures 1H and S3).

Optogenetic activation of MeApd elicited intense, time-locked attack towards intruder males, castrated males, and females (Figure 1I–J, Movie S1). To reliably measure the level of time-locked activation of attack that is induced by optogenetic stimulation, we minimized the baseline aggression level by group housing resident animals prior to the virus injection and fiber implantation (see Methods). In these ChR2-expressing males, attack was triggered towards male intruders in 100% of ChR2-expressing animals and over 60% of the trials; attack was also triggered towards castrated males and female intruders (Figures 1K–1L). Attack evoked by optogenetic stimulation included both biting and tussling (Movie S1), similar to the pattern of naturally occurring attack behavior in unmanipulated animals (Kruk, 1991; Kruk et al., 1998; Siegel et al., 1999). Furthermore, attack was initiated at the onset and ceased after the offset of photostimulation, with short latencies (Figures 1M–1N). Episodes of attack occupied 45–60% of the photostimulation period (Figure 1O). Animals expressing a control EYFP virus in MeApd failed to show any photostimulation-evoked aggression (Figures 1I, 1K, 1L, and 1O). These data indicate that activation of MeApd neurons using a generic promoter can promote aggression.

GABAergic neurons in MeApd promote aggressive behavior

To determine whether attack can be triggered by optogenetic stimulation of a specific, genetically defined population within MeApd, we sought to identify lines of Cre recombinase-expressing mice that could be used to manipulate distinct subsets of MeApd neurons. MeApd consists of both $vGAT^+$ (GABAergic) and $vGLUT2^+$ (glutamatergic) neurons (Choi et al., 2005), but they are differentially distributed along the medio-lateral axis: $vGAT^+$ neurons are distributed throughout MeApd whereas $vGLUT2^+$ neurons are preferentially enriched in the medial region (Bian et al., 2007) (Figures 2A–2D). We therefore investigated whether GABAergic and/or glutamatergic neurons might contain aggression-promoting cells.

We first asked whether GABAergic and/or glutamatergic neurons are activated during attack, using c-fos induction. Existing antibodies to GABAergic markers do not provide cellular resolution in the MeA (data not shown), precluding a quantitative comparison with c-fos expression. Therefore, we generated double heterozygous male mice that expressed both vGAT-Cre (Vong et al., 2011) and a Cre-dependent reporter ZsGreen (Ai6) (Madisen et al., 2010), which provides strong cell body labeling. Double labeling for c-fos and ZsGreen in males that had recently attacked an intruder (Figures 2A–2D) revealed, surprisingly, that more than 90% of the $c\text{-}fos^+$ neurons were $ZsGreen^+$, suggesting the majority of $c\text{-}fos^+$ neurons induced by attack are $vGAT^+$ (Figures 2A–2B, 2E). In contrast, in double-transgenic animals that expressed vGLUT2-Cre and ZsGreen, <10% of the $c\text{-}fos^+$

neurons were ZsGreen^{+} following attack (Figures 2C–2E). Furthermore, ~30% of the vGAT^{+} neurons were c-fos^{+}, whereas ~3% of the vGLUT2^{+} neurons were c-fos^{+} (Figure S2E). In control animals that did not experience social interactions, little overlap was observed between c-fos^{+} and ZsGreen^{+} neurons (data not shown). These data suggest that neurons in MeApd that are activated during attack behavior are predominantly vGAT^{+}.

To determine whether attack could be triggered by optogenetic activation of GABAergic neurons in MeApd, we injected vGAT$^{Cre/+}$ male mice with a rAAV virus encoding a Cre-dependent ChR2 (Figures 2F, S2B). Whole-cell patch clamp recordings in acute MeA brain slices confirmed that photostimulation elicited action potentials from ChR2-expressing vGAT^{+} cells with high fidelity (Figures 2G–2I). Successful photostimulation of ChR2-expressing vGAT^{+} neurons *in vivo* via an implanted optic fiber was confirmed by double labeling for hrGFP and c-fos (Figures 2J–2L).

Optogenetic stimulation of vGAT^{+} neurons in MeApd triggered intense attack in all ChR2-expressing animals (Figures 2M–2N, Movie S2). Attack was triggered towards male intruders in over 90% of the trials and towards castrated males and female intruders in 75–80% of the trials (Figure 2O), with short latency relative to the onset of photostimulation (Figures 2P–2Q). When light pulses were delivered under optimal conditions (the resident facing the intruder and within half a body-length (Lee et al., 2014; Lin et al., 2011)), attack was triggered within ~1s of photostimulation (Figure 2Q). Attack, on average, lasted 60–85% of the stimulation period (Figure 2R). Photostimulation of MeApd GABAergic neurons also evoked attack towards a toy mouse (Figure 2S), suggesting that olfactory cues are not essential for optogenetically evoked aggression, and also that attack is not due to a defect in sex discrimination (Lee et al., 2014; Lin et al., 2011).

GABAergic neuron activity in MeApd is required for ongoing aggressive behavior

We next addressed the requirement of MeApd vGAT^{+} neuronal activity for aggression in a time-resolved manner, via optogenetic inhibition using a Cre-dependent rAAV encoding eNpHR3, a light-driven chloride pump (Gradinaru et al., 2010), in vGAT$^{Cre/+}$ male mice (Figures 3A, S2D). Efficient photostimulation-dependent (593 nm) silencing of vGAT^{+} neurons was confirmed by whole-cell patch clamp recording in acute MeApd brain slices prepared from virally injected animals (Figures 3B–3C).

We examined the behavioral effects of optogenetically silencing MeApd vGAT^{+} neurons (Figures 3D–3E). To reliably examine time-resolved suppression of attack, we pre-selected resident animals with higher levels of baseline attack based on pilot resident-intruder trials without photostimulation (see Methods). Photostimulation of a resident mouse in its home cage was applied for 3 s, after the onset of spontaneous aggressive encounters with a male intruder. In response to optogenetic inhibition, males stopped attacking in <1 s in 97% of the photostimulation trials, with an average latency <0.5 s (Figures 3E–3J, Movie S3). Similarly, optogenetic silencing of MeApd neurons in wild-type mice using a generic EF1α promoter-driven eNpHR3 also interrupted attack (Figures 3F, 3I, 3J and S4). In contrast, control males expressing EYFP continued to attack the intruder in over 90% of stimulation trials (Figures 3E–3G and 3I–3J). These data indicated that ongoing activity in MeApd vGAT^{+} neurons is required for naturally occurring attack behavior.

GABAergic neurons control different social behaviors at different stimulation intensities

The foregoing data indicated that vGAT^{+} neurons in MeApd are both necessary and sufficient for aggressive behavior. We next asked whether MeApd vGAT^{+} neurons could also promote other social behaviors. Our previous studies showed that photostimulation of VMHvl neurons at different light intensities triggered different social behaviors: low intensity photostimulation triggered sniffing and mounting behavior, while high intensity photostimulation triggered attack (Lee et al., 2014). To determine whether this phenomenon is also characteristic of MeApd, we performed optogenetic stimulation of vGAT^{+} neurons across a wide range of illumination intensities (Figure 4A). Indeed, low intensity stimulation triggered mounting behavior towards intact and castrated males, as well as female intruders (Figures 4A–4B, Movie S4). As the intensity of stimulation was increased, evoked behaviors in the same animals switched from mounting to attack (Figures 4C–4D). At intermediate light intensities, photostimulation triggered a mixture of attack and mounting behavior (Figure 4A).

Interestingly, low intensity stimulation of MeApd vGAT^{+} neurons also triggered social grooming behavior towards intact and castrated males (Figures 4B and 4E), a behavior not observed in the VMHvl-stimulated animals (Lee et al., 2014). As the light intensity was increased, we observed a transition from social grooming to attack in the same mice (Figures 4F–4G). Interestingly, low intensity stimulation triggered social grooming in some animals, and mounting in other animals. Attempts to separate these behaviors by systematically manipulating stereotaxic injection coordinates within MeApd were unsuccessful (data not shown). Together, these data indicate that optogenetic activation of vGAT^{+} neurons in MeApd, as in VMHvl (Lee et al., 2014), can promote multiple social behaviors in an intensity-dependent manner.

Neighboring glutamatergic neurons promote self-grooming behavior

The foregoing data indicated that vGAT^{+} neurons in MeApd can promote multiple social behaviors. This observation raised the question of whether other subpopulations of MeApd neurons would also promote such social behaviors. Since MeApd contains both glutamatergic and GABAergic neurons (Figure 2A–D), we next targeted the glutamatergic population marked by expression of vGLUT2.

We injected vGLUT2$^{Cre/+}$ male mice (Vong et al., 2011) with an rAAV virus encoding a Cre-dependent ChR2 (Figures 5A, S2C). Whole-cell patch clamp recordings in acute MeApd brain slices confirmed that photostimulation elicited action potentials from ChR2-expressing vGLUT2^{+} cells with high temporal precision and high spike fidelity (Figures 5B–5D). Successful photostimulation of vGLUT2^{+} neurons *in vivo* via an implanted optic fiber was confirmed by double labeling for hrGFP and c-fos (Figures 5E–5G).

We then examined behaviorally the effect of optogenetic stimulation of vGLUT2^{+} neurons in resident mice exposed to an intruder. Interestingly, photostimulation did not elicit any attack, mounting, or social grooming behavior in the presence of an intruder of any sex (Figures 5H–5J). Instead, photostimulation elicited robust, repetitive self-grooming behavior with short latency in all ChR2-expressing vGLUT2$^{Cre/+}$ animals tested (Figures 5H–5L,

5N). Self-grooming behavior was also observed when stimulation was applied to solitary animals (Figures 5H and 5M–5N). The self-grooming behavior evoked by optogenetic stimulation consisted of paw licking, facial grooming as well as body grooming (Movie S5), similar to the pattern of spontaneous self-grooming behavior in wild type animals. Importantly, optogenetic stimulation of vGLUT2$^+$ neurons did not evoke any other non-social behaviors, such as locomotion, freezing, jumping, feeding or drinking. Finally, self-grooming behavior was not triggered by inhibition of naturally occurring attack via optogenetic silencing of vGAT$^+$ neurons (Figure S6E), or during the offset of optogenetically activated aggression, arguing that this repetitive behavior is not simply a default activity that invariably occurs when an ongoing social behavior such as aggression is interrupted.

Interestingly, the self-grooming behavior triggered by the activation of vGLUT2$^+$ neurons persisted for several seconds after the termination of the stimulation (Figures 5L and 5O). The persistent effect was greater in solitary animals when no intruder was present (Figures 5M and 5O). Whether this persistence reflects a persistent internal brain state, or is promoted by positively reinforcing sensory feedback, is not yet clear.

The effect of optogenetic activation to trigger self-grooming was also highly specific to vGLUT2$^+$ neurons, as stimulation of vGAT$^+$ neurons did not trigger any self-grooming behavior (Figures 5I–5J). Interestingly, when MeApd neurons were photostimulated with ChR2 expressed non-selectively in wild type animals (see Figure 1E), a mixture of both attack and repetitive self-grooming was observed (Figures 5I–5J). The elicitation of both behaviors at a single injection site using a ubiquitous promoter likely reflects a co-activation of both GABAergic and glutamatergic neurons, emphasizing the functional heterogeneity of MeApd.

When ChR2 virus was injected into MeApd, its expression occasionally spread into the adjacent lateral hypothalamic area (LHA), a small region medial to MeApd (Figure S5). To determine whether there is any spatial specificity within MeApd and adjacent LHA in triggering different behaviors, ChR2 virus was injected into different locations in MeApd and adjacent LHA using modified stereotaxic coordinates (see Methods). The anatomical distribution of ChR2-expressing neurons in these injected animals is illustrated in Figure S5D. These studies indicated that the vGAT$^+$ neurons that trigger attack are located within the MeApd (Figure S5E). Self-grooming could be triggered when the majority of ChR2-expressing vGLUT2$^+$ neurons are located in MeApd (Figure S5F). It could also be triggered, to a lesser extent, by injections into the lateral part of LHA (Figure S5F). Thus the excitatory neurons that promote self-grooming are interspersed and/or juxtaposed with the inhibitory neurons that promote social behaviors.

Glutamatergic neurons suppress social behaviors

Because activation of glutamatergic neurons promoted repetitive self-grooming, we next examined whether optogenetic stimulation of vGLUT2$^+$ neurons during an ongoing social behavior would interrupt the latter in a dominant manner. Indeed, stimulation of ChR2-expressing vGLUT2$^+$ MeApd neurons interrupted naturally occurring attack in less than 3 s, in over 75% of the stimulation trials (Figures 6A–6E). Similarly, optogenetic activation of

these glutamatergic neurons also suppressed naturally occurring mounting behavior towards a female (Figures 6A, 6F–6H).

The suppression of social behaviors by glutamatergic neurons could be explained by two alternative hypotheses: (1) simple physical incompatibility with evoked self-grooming behavior that dominates spontaneous social behavior (Figure 6I, upper); or (2) direct inhibition of social behaviors that is not causally related to the promotion of self-grooming (Figure 6I, lower). During stimulation of vGLUT2$^+$ neurons, the interruption of ongoing attack occurred prior to the onset of self-grooming, with an average delay of 4.6±0.8 s; a similar average delay of 5.3±0.6 s was observed for the interruption of mounting (Figure 6J). Thus, the interruption of ongoing social behavior preceded the onset of self-grooming following activation of glutamatergic neurons, arguing that these neurons independently suppress social behavior.

To investigate this issue further, we performed long-term pharmacogenetic activation of vGLUT2$^+$ neurons in MeApd using a Cre-dependent virus encoding the activating DREADD hM3D and an mCherry fluorescent marker (Alexander et al., 2009) (Figure 6L). Successful pharmacogenetic activation of vGLUT2$^+$ neurons via injection of the specific ligand CNO was confirmed by double labeling for mCherry and c-fos (Figure S6A–B). Interestingly, pharmacogenetic activation of vGLUT2$^+$ neurons resulted in a marked reduction of social interactions (from ~400 s to ~200 s) (Figures 6K, 6M, 6N). In contrast, this manipulation did not reduce interactions with novel objects (Figure S6D), suggesting that it did not promote a state of anxiety. Importantly, under these conditions, self-grooming was only sporadically evoked and occupied only ~20 s of the total observation period (Figure S6C), which cannot account for the duration and total extent of reduced social interactions. These data demonstrate that activation of vGLUT2$^+$ neurons in MeApd causes an active suppression of social interactions, independently of its effect to promote self-grooming behavior. Together, the foregoing results indicate that GABAergic and glutamatergic neurons in MeApd exert antagonistic influences to promote and inhibit social behaviors, respectively.

GABAergic Neurons Suppress Naturally Occurring Self-grooming

The observation that MeApd glutamatergic neurons actively inhibit social behaviors prompted us to ask whether activation of the vGAT$^+$ population might, conversely, inhibit self-grooming behavior. Indeed, optogenetic activation of vGAT$^+$ neurons acutely interrupted ongoing, spontaneous self-grooming behavior (Figure 7A, Movie S6), in a manner time-locked to the onset of photostimulation. This suppression could reflect (1) an indirect inhibition due to promotion of attack (Figure 7B, upper); or (2) a parallel influence to inhibit self-grooming that is independent of the promotion of social behavior (Figure 7B, lower).

To distinguish between these possibilities, we optogenetically activated MeApd vGAT$^+$ neurons in solitary animals in their home cage. Under these conditions, photostimulation-dependent suppression of self-grooming was observed in animals performing spontaneous bouts of self-grooming (Figures 7A, 7C). Self-grooming was interrupted in less than 2 s following the onset of stimulation in over 95% of trials (Figures 7C–7F). This interruption

of grooming was not observed in EYFP-expressing animals (Figures 7A, 7D–7F). Because no intruder animal was present in the cage, this inhibition of self-grooming cannot be explained by physical incompatibility with social behaviors promoted by $vGAT^+$ neuron activation. Thus, our evidence indicates that MeApd GABAergic neurons exert an influence to suppress self-grooming, independently of their function to promote social behaviors.

To examine whether activation of MeApd $vGAT^+$ neurons might generally suppress any non-social goal-oriented behavior, we also investigated the influence of $vGAT^+$ neurons on feeding behavior. Optogenetic activation of $vGAT^+$ neurons did not inhibit ongoing feeding behavior (Figures 7G–7K). Although we cannot exclude that other solitary behaviors might be inhibited by GABAergic neuron activation, at the very least these data indicate that $vGAT^+$ neurons do not suppress any type of non-social behavior, suggesting a specific inhibitory influence on self-grooming.

DISCUSSION

Using cell-type specific functional manipulations, we identified two non-overlapping neuronal subpopulations in MeApd that promote social and non-social behaviors. GABAergic MeApd neurons promoted three different social behaviors in an intensity-dependent manner: aggression, mating and social grooming. In contrast, neighboring glutamatergic neurons in MeApd and adjacent LHA promoted repetitive self-grooming, an asocial behavior. This glutamatergic subpopulation also inhibited social behaviors, independently of its effect to promote self-grooming. Conversely, MeApd GABAergic neurons suppressed self-grooming, in both paired and solitary animals. Together, these data suggest that inhibitory and excitatory MeApd subpopulations control social behaviors vs. repetitive self-grooming, respectively, in an antagonistic manner. These data provide new insights into the circuit-level control of opponent innate behaviors by the MeA.

MeApd GABAergic neurons promote aggression

The MeA is activated by chemosensory cues and relays this information through complex circuitry that involves connections with the bed nucleus of the stria terminalis (BNST) and the medial hypothalamus (Choi et al., 2005; Dong et al., 2001; Swanson, 2000). It has been proposed, based on c-fos activation and lesion studies, that this circuit is subdivided into topographically segregated pathways that control defensive vs. reproductive (sexual) behaviors (Canteras et al., 1995; Swanson, 2000). According to this hodological scheme, MeApd is associated with reproductive behaviors and MeApv with defensive behaviors.

How the control of aggression fits into this scheme has not been clear, as aggression has both defensive and offensive forms (Blanchard et al., 2003). Our data provide definitive evidence that the MeApd activity is both necessary and sufficient for inter-male offensive aggression. Our data further demonstrate that the aggression-promoting neurons in MeApd are GABAergic, while glutamatergic neurons inhibit aggression. These data may explain in part why previous lesion studies of MeA have yielded contradictory results (Busch and Barfield, 1974; Kemble et al., 1984; Rosvold et al., 1954; Takahashi and Gladstone, 1988; Vochteloo and Koolhaas, 1987; Wang et al., 2013). Since VMHvl attack neurons are likely glutamatergic (Choi et al., 2005; Lin et al., 2011), it seems probable that MeApd

GABAergic neurons promote aggression via dis-inhibition of these glutamatergic neurons. Functional studies will be required to identify potential dis-inhibition site(s).

Scalable control of social behaviors in MeApd

Recent studies have revealed that $Esr1^+$ neurons in VMHvl (also expressing the progesterone receptor (Yang et al., 2013)) control multiple social behaviors in an intensity-dependent manner: stronger optogenetic stimulation evokes attack whereas weaker optogenetic stimulation elicits social investigation and mounting (Lee et al., 2014). Our finding that $vGAT^+$ neurons in MeApd control multiple social behaviors in a scalable manner echoes these observations, and suggests that this scalable control of social behavior may already emerge at the level of MeApd. Alternatively, it may reflect feedback from VMHvl (Canteras et al., 1994). Several models can explain how such an intensity coding of social behavior is implemented at the cellular level, including different populations of neurons with different activation thresholds, or graded changes in activity within a single population (Lee et al., 2014). Distinguishing between these mechanisms, and the locations(s) at which they are implemented, will be an important topic for future investigation.

Antagonistic control of self-grooming and social behaviors in MeApd

It is striking that MeA neurons that promote self-grooming can be cleanly separated from those that promote social behaviors, along the axis of excitatory vs. inhibitory neurons, respectively. Self-grooming has traditionally been associated with paraventricular hypothalamic nuclei distinct from regions that control social behaviors (Kruk et al., 1998). Self-grooming can be observed in a variety of contexts, and may express different internal states of both positive and negative valence (Tinbergen, 1951). The internal drives or motivations associated with the repetitive self-grooming elicited in these experiments are not clear, and could reflect anxiogenic, anxiolytic, social avoidance or other states. The fact that activation of $vGLUT2^+$ neurons in MeApd and adjacent LHA elicits self-grooming, but not other activities such as feeding, drinking, freezing, flight, digging or nesting, suggests that the influence of these neurons is specific for this repetitive asocial behavior.

Our experiments further reveal that these two MeA subpopulations not only control self-grooming and social behavior in a mutually exclusive and positive-acting manner, but that they also each play a negative-acting role to inhibit the behavior promoted by the other: the GABAergic neurons inhibit self-grooming, while the glutamatergic neurons inhibit social behaviors (Figure S7). Importantly, the observed reciprocal inhibitory effects do not reflect simple physical incompatibility between behaviors promoted in a positive-acting manner, but rather reflect an independent, negative-acting function for both neuronal subpopulations. Identification of the site(s) and synaptic mechanisms underlying such reciprocal antagonism will be an important topic for future study.

Potential relevance to psychiatric disorders affecting social interactions

Abnormalities in social behaviors have been observed in several psychiatric disorders, including autism and schizophrenia (Couture et al., 2010; Sasson et al., 2007). Impaired social interactions are a major symptom of autism, for example, and are a signature phenotype in many mouse models of this disorder (Silverman et al., 2010; Williams, 2008).

A prominent hypothesis, the “excitation:inhibition imbalance hypothesis,” posits that autism may be caused by an increase in the relative level of excitation vs. inhibition in multiple brain regions (Markram and Markram, 2010; Rubenstein and Merzenich, 2003). In that context, it is striking that social interactions were strongly inhibited by increasing the level of excitatory neuronal activity in the amygdala, a structure whose dysfunction has been implicated in autism (Baron-Cohen et al., 2000; Birmingham et al., 2011). Such manipulations, moreover, also promoted repetitive self-grooming, a behavioral phenotype seen in some genetic mouse models of autism as well (Blundell et al., 2010; Etherton et al., 2009; Silverman et al., 2010). Conversely, activation of amygdala GABAergic neurons promoted social behaviors and inhibited self-grooming. These unexpected findings suggest that this system may prove useful for investigating further how alterations in the relative levels of excitatory vs. inhibitory neuronal activity in the amygdala can influence the “decision” to engage in social vs. repetitive asocial behaviors. They may also suggest candidate neural substrates for gene variants implicated in psychiatric disorders that affect social interactions in humans (Fatemi et al., 2002; Jamain et al., 2002).

EXPERIMENTAL PROCEDURES

Experimental Subjects

Subjects were wild type C57BL/6N (Charles River), vGAT$^{Cre/+}$, or vGLUT2$^{Cre/+}$ male mice (Vong et al., 2011). Intruder mice were BALB/c or C57BL/6N males (intact and castrated) and BALB/c females, purchased at 8 weeks old (Charles River). Care and experimental manipulations of animals were in accordance with the NIH Guide for Care and Use of Laboratory Animals and approved by the Caltech Institutional Animal Care and Use Committee.

Stereotaxic Surgery, Virus Injection, and Optic-fiber Placement

Mice at 8 weeks old were anaesthetized with isofluorane and mounted in a stereotaxic apparatus (Kopf Instruments). In all experiments except for Figure S5, viruses were injected bilaterally into MeApd (ML ±2.00, AP −1.50, DV −5.15 from bregma). In Figure S5, viruses were injected using slightly different stereotaxic coordinates along the mediolateral axis (ML between ±1.60 and ±2.10, AP −1.50, DV −5.15 from bregma). Injections were carried out using a pulled, fine glass capillary at a rate of 30 nl min^{-1} for a total volume of 300 nl. A custom made ferrule fiber (200 μm in core diameter, Doric Lenses) was subsequently placed at 0.5 mm above the virus injection site in the target brain area, and fixed on the skull with dental cement (Parkell; Metabond). In all experiments the virus was allowed 3–4 weeks to incubate before behavioral testing or perfusion. Unless otherwise indicated, all control animals used in this study were animals with the same genetic background injected with viruses expressing EYFP.

Optogenetic Activation and Silencing

Wild type, vGLUT2$^{Cre/+}$, or vGLUT2$^{Cre/+}$ mice at 8 weeks old were injected bilaterally into MeApd with a rAAV expressing ChR2 or eNpHR3 and bilaterally implanted with optic fibers. After a 3–4-week recovery period, the virus-injected animals were subject to behavioral testing in their home cage for 2 to 4 weeks. Photostimulation (ChR2, 473 nm, 20

Hz, 20 ms pulses, 1–3 mW mm^{-2}; or eNpHR3, 593 nm, continuous, 1–3 mW mm^{-2}) was administered to mice in the absence or presence of an intruder mouse.

Pharmacogenetic activation

vGLUT2$^{Cre/+}$ mice at 8 weeks old were injected bilaterally into MeApd with a Cre-dependent rAAV expressing the pharmacogenetic activator DREADD hM3D (AAV2-EF1α-DIO-hM3D-mCherry). The virus was allowed 4 weeks to incubate before behavioral testing. CNO (Clozapine N-oxide, 1.5 mg/kg, Enzo Life Sciences) or saline was administrated by intraperitoneal injection. 30 mins after the CNO or saline administration, animals were transferred in their home cage to a behavioral testing room and were tested for social interaction and self-grooming.

Behavioral Testing

Aggression was examined using the resident-intruder assay. Housing conditions prior to surgery were selected depending on the level of baseline aggression appropriate for activation (low baseline) vs. inhibition (high baseline) experiments. A more submissive mouse was used as the intruder male in all the experiments; all resident animals included in the study initiated all the attacks during the aggression test. See Extended Experimental Procedures for additional behavioral tests.

Additional Methods

Detailed methods on experimental subjects, viral vectors, behavioral assays, behavior equipment setup, video acquisition and analysis, optogenetic stimulation, acute slice electrophysiology, and immunohistochemistry can be found in the Extended Experimental Procedures.

Supplementary Material

Refer to Web version on PubMed Central for supplementary material.

Acknowledgments

We thank X. Wang, X. Da, M. McCardle, R. Robertson, and C. Park for technical assistance, T. Anthony for the ChR2 virus, the Caltech GEMS and animal facility for maintaining mice, M. Zelikowsky, H. Cai, and K. Asahina for commenting on the manuscript, and members of the Anderson lab for discussions. W.H. is a Helen Hey Whitney Fellow. D.J.A. is a Howard Hughes Medical Institute Investigator and a Paul G. Allen Distinguished Investigator. This work was supported in part by NIH Grants No. MH085082 and MH070053, and a grant from the Simons Foundation.

References

Adams DB. Brain mechanisms of aggressive behavior: an updated review. Neuroscience and biobehavioral reviews. 2006; 30:304–318. [PubMed: 16289283]

Alexander GM, Rogan SC, Abbas AI, Armbruster BN, Pei Y, Allen JA, Nonneman RJ, Hartmann J, Moy SS, Nicolelis MA, et al. Remote control of neuronal activity in transgenic mice expressing evolved G protein-coupled receptors. Neuron. 2009; 63:27–39. [PubMed: 19607790]

Aravanis AM, Wang LP, Zhang F, Meltzer LA, Mogri MZ, Schneider MB, Deisseroth K. An optical neural interface: in vivo control of rodent motor cortex with integrated fiberoptic and optogenetic technology. Journal of neural engineering. 2007; 4:S143–S156. [PubMed: 17873414]

Baron-Cohen S, Ring HA, Bullmore ET, Wheelwright S, Ashwin C, Williams SC. The amygdala theory of autism. Neuroscience and biobehavioral reviews. 2000; 24:355–364. [PubMed: 10781695]

Bergan JF, Ben-Shaul Y, Dulac C, Mason P. Sex-specific processing of social cues in the medial amygdala. eLife. 2014:3.

Bian X, Yanagawa Y, Chen WR, Luo M. Cortical-Like Functional Organization of the Pheromone-Processing Circuits in the Medial Amygdala. Journal of neurophysiology. 2007; 99:77–86. [PubMed: 17977926]

Birmingham E, Cerf M, Adolphs R. Comparing social attention in autism and amygdala lesions: effects of stimulus and task condition. Soc Neurosci. 2011; 6:420–435. [PubMed: 21943103]

Blanchard RJ, Wall PM, Blanchard DC. Problems in the study of rodent aggression. Hormones and behavior. 2003; 44:161–170. [PubMed: 14609538]

Blundell J, Blaiss CA, Etherton MR, Espinosa F, Tabuchi K, Walz C, Bolliger MF, Südhof TC, Powell CM. Neuroligin-1 deletion results in impaired spatial memory and increased repetitive behavior. The Journal of neuroscience : the official journal of the Society for Neuroscience. 2010; 30:2115–2129. [PubMed: 20147539]

Boyden ES, Zhang F, Bamberg E, Nagel G, Deisseroth K. Millisecond-timescale, genetically targeted optical control of neural activity. Nature Neuroscience. 2005; 8:1263–1268.

Busch DE, Barfield RJ. A failure of amygdaloid lesions to alter agonistic behavior in the laboratory rat. Physiology & behavior. 1974; 12:887–892. [PubMed: 4600066]

Canteras NS, Simerly RB, Swanson LW. Organization of projections from the ventromedial nucleus of the hypothalamus: a Phaseolus vulgaris-leucoagglutinin study in the rat. J Comp Neurol. 1994; 348:41–79. [PubMed: 7814684]

Canteras NS, Simerly RB, Swanson LW. Organization of projections from the medial nucleus of the amygdala: a PHAL study in the rat. The Journal of Comparative Neurology. 1995; 360:213–245. [PubMed: 8522644]

Chamero P, Marton TF, Logan DW, Flanagan K, Cruz JR, Saghatelian A, Cravatt BF, Stowers L. Identification of protein pheromones that promote aggressive behaviour. Nature. 2007; 450:899–902. [PubMed: 18064011]

Choi GB, Dong HW, Murphy AJ, Valenzuela DM, Yancopoulos GD, Swanson LW, Anderson DJ. Lhx6 delineates a pathway mediating innate reproductive behaviors from the amygdala to the hypothalamus. Neuron. 2005; 46:647–660. [PubMed: 15944132]

Couture SM, Penn DL, Losh M, Adolphs R, Hurley R, Piven J. Comparison of social cognitive functioning in schizophrenia and high functioning autism: more convergence than divergence. Psychol Med. 2010; 40:569–579. [PubMed: 19671209]

Dhungel S, Masaoka M, Rai D, Kondo Y, Sakuma Y. Both olfactory epithelial and vomeronasal inputs are essential for activation of the medial amygdala and preoptic neurons of male rats. Neuroscience. 2011; 199:225–234. [PubMed: 21983295]

Dong HW, Petrovich GD, Swanson LW. Topography of projections from amygdala to bed nuclei of the stria terminalis. Brain research Brain research reviews. 2001; 38:192–246. [PubMed: 11750933]

Dulac C, Torello AT. Molecular detection of pheromone signals in mammals: from genes to behaviour. Nature Reviews Neuroscience. 2003; 4:551–562.

Duvarci S, Pare D. Amygdala Microcircuits Controlling Learned Fear. Neuron. 2014; 82:966–980. [PubMed: 24908482]

Ehrlich I, Humeau Y, Grenier F, Ciocchi S, Herry C, Lüthi A. Amygdala inhibitory circuits and the control of fear memory. Neuron. 2009; 62:757–771. [PubMed: 19555645]

Erskine MS. Mating-induced increases in FOS protein in preoptic area and medial amygdala of cycling female rats. Brain research bulletin. 1993; 32:447–451. [PubMed: 8221135]

Etherton MR, Blaiss CA, Powell CM, Südhof TC. Mouse neurexin-1alpha deletion causes correlated electrophysiological and behavioral changes consistent with cognitive impairments. Proceedings of the National Academy of Sciences. 2009; 106:17998–18003.

Fatemi SH, Halt AR, Stary JM, Kanodia R, Schulz SC, Realmuto GR. Glutamic acid decarboxylase 65 and 67 kDa proteins are reduced in autistic parietal and cerebellar cortices. Biological psychiatry. 2002; 52:805–810. [PubMed: 12372652]

Gradinaru V, Zhang F, Ramakrishnan C, Mattis J, Prakash R, Diester I, Goshen I, Thompson KR, Deisseroth K. Molecular and cellular approaches for diversifying and extending optogenetics. Cell. 2010; 141:154–165. [PubMed: 20303157]

Jamain S, Betancur C, Quach H, Philippe A, Fellous M, Giros B, Gillberg C, Leboyer M, Bourgeron T, Study PARISP. Linkage and association of the glutamate receptor 6 gene with autism. Molecular psychiatry. 2002; 7:302–310. [PubMed: 11920157]

Kemble ED, Blanchard DC, Blanchard RJ, Takushi R. Taming in wild rats following medial amygdaloid lesions. Physiology & behavior. 1984; 32:131–134. [PubMed: 6538976]

Kollack SS, Newman SW. Mating behavior induces selective expression of Fos protein within the chemosensory pathways of the male Syrian hamster brain. Neuroscience letters. 1992; 143:223–228. [PubMed: 1436670]

Kollack-Walker S, Newman SW. Mating and agonistic behavior produce different patterns of Fos immunolabeling in the male Syrian hamster brain. Neuroscience. 1995; 66:721–736. [PubMed: 7644033]

Kondo Y. Lesions of the medial amygdala produce severe impairment of copulatory behavior in sexually inexperienced male rats. Physiology & behavior. 1992; 51:939–943. [PubMed: 1615054]

Kondo Y, Arai Y. Functional association between the medial amygdala and the medial preoptic area in regulation of mating behavior in the male rat. Physiology & behavior. 1995; 57:69–73. [PubMed: 7878127]

Kruk MR. Ethology and pharmacology of hypothalamic aggression in the rat. Neurosci Biobehav Rev. 1991; 15:527–538. [PubMed: 1792015]

Kruk MR, Westphal KG, Van Erp AM, van Asperen J, Cave BJ, Slater E, de Koning J, Haller J. The hypothalamus: cross-roads of endocrine and behavioural regulation in grooming and aggression. Neuroscience & Biobehavioral Reviews. 1998; 23:163–177. [PubMed: 9884110]

Lee H, Kim DW, Remedios R, Anthony TE, Chang A, Madisen L, Zeng H, Anderson DJ. Scalable control of mounting and attack by Esr1+ neurons in the ventromedial hypothalamus. Nature. 2014; 509:627–632. [PubMed: 24739975]

Lehman MN, Winans SS, Powers JB. Medial nucleus of the amygdala mediates chemosensory control of male hamster sexual behavior. Science. 1980; 210:557–560. [PubMed: 7423209]

Lin D, Boyle MP, Dollar P, Lee H, Lein ES, Perona P, Anderson DJ. Functional identification of an aggression locus in the mouse hypothalamus. Nature. 2011; 470:221–226. [PubMed: 21307935]

Madisen L, Zwingman TA, Sunkin SM, Oh SW, Zariwala HA, Gu H, Ng LL, Palmiter RD, Hawrylycz MJ, Jones AR, et al. A robust and high-throughput Cre reporting and characterization system for the whole mouse brain. Nat Neurosci. 2010; 13:133–140. [PubMed: 20023653]

Mandiyan VS, Coats JK, Shah NM. Deficits in sexual and aggressive behaviors in Cnga2 mutant mice. Nature Neuroscience. 2005; 8:1660–1662.

Markram K, Markram H. The intense world theory - a unifying theory of the neurobiology of autism. Front Hum Neurosci. 2010; 4:224. [PubMed: 21191475]

Nelson RJ, Trainor BC. Neural mechanisms of aggression. Nature Reviews Neuroscience. 2007; 8:536–546.

Newman SW. The medial extended amygdala in male reproductive behavior a node in the mammalian social behavior network. Annals of the New York Academy of Sciences. 1999; 877:242–257. [PubMed: 10415653]

Niimi K, Horie S, Yokosuka M, Kawakami-Mori F, Tanaka K, Fukayama H, Sahara Y. Heterogeneous electrophysiological and morphological properties of neurons in the mouse medial amygdala in vitro. Brain research. 2012; 1480:41–52. [PubMed: 22960119]

Paré D, Quirk GJ, LeDoux JE. New vistas on amygdala networks in conditioned fear. J Neurophysiol. 2004; 92:1–9. [PubMed: 15212433]

Pitkänen A, Savander V, LeDoux JE. Organization of intra-amygdaloid circuitries in the rat: an emerging framework for understanding functions of the amygdala. Trends Neurosci. 1997; 20:517–523. [PubMed: 9364666]

Rosvold HE, Mirsky AF, Pribram KH. Influence of amygdalectomy on social behavior in monkeys. Journal of comparative and physiological psychology. 1954; 47:173–178. [PubMed: 13163250]

Rubenstein JLR, Merzenich MM. Model of autism: increased ratio of excitation/inhibition in key neural systems. Genes, brain, and behavior. 2003; 2:255–267.

Sasson N, Tsuchiya N, Hurley R, Couture SM, Penn DL, Adolphs R, Piven J. Orienting to social stimuli differentiates social cognitive impairment in autism and schizophrenia. Neuropsychologia. 2007; 45:2580–2588. [PubMed: 17459428]

Siegel A, Roeling TA, Gregg TR, Kruk MR. Neuropharmacology of brain-stimulation-evoked aggression. Neuroscience and biobehavioral reviews. 1999; 23:359–389. [PubMed: 9989425]

Silverman JL, Yang M, Lord C, Crawley JN. Behavioural phenotyping assays for mouse models of autism. Nature Reviews Neuroscience. 2010; 11:490–502.

Stanley DA, Adolphs R. Toward a neural basis for social behavior. Neuron. 2013; 80:816–826. [PubMed: 24183030]

Stowers L, Holy TE, Meister M, Dulac C, Koentges G. Loss of sex discrimination and male-male aggression in mice deficient for TRP2. Science. 2002; 295:1493–1500. [PubMed: 11823606]

Swanson LW. Cerebral hemisphere regulation of motivated behavior. Brain research. 2000; 886:113–164. [PubMed: 11119693]

Swanson LW, Petrovich GD. What is the amygdala? Trends in neurosciences. 1998; 21:323–331. [PubMed: 9720596]

Takahashi LK, Gladstone CD. Medial amygdaloid lesions and the regulation of sociosexual behavioral patterns across the estrous cycle in female golden hamsters. Behavioral neuroscience. 1988; 102:268–275. [PubMed: 3365322]

Tinbergen, N. The study of instinct. New York, NY: Clarendon Press/Oxford University Press; 1951.

Veening JG, Coolen LM, de Jong TR, Joosten HW, de Boer SF, Koolhaas JM, Olivier B. Do similar neural systems subserve aggressive and sexual behaviour in male rats? Insights from c-Fos and pharmacological studies. European journal of pharmacology. 2005; 526:226–239. [PubMed: 16263109]

Vochteloo JD, Koolhaas JM. Medial amygdala lesions in male rats reduce aggressive behavior: interference with experience. Physiology & behavior. 1987; 41:99–102. [PubMed: 3685168]

Vong L, Ye C, Yang Z, Choi B, Chua J, Streamson and, Lowell BB. Leptin Action on GABAergic Neurons Prevents Obesity and Reduces Inhibitory Tone to POMC Neurons. Neuron. 2011; 71:142–154. [PubMed: 21745644]

Wang Y, He Z, Zhao C, Li L. Medial amygdala lesions modify aggressive behavior and immediate early gene expression in oxytocin and vasopressin neurons during intermale exposure. Behavioural brain research. 2013

Williams JH. Self-other relations in social development and autism: multiple roles for mirror neurons and other brain bases. Autism Res. 2008; 1:73–90. [PubMed: 19360654]

Xu X, Coats JK, Yang CF, Wang A, Ahmed OM, Alvarado M, Izumi T, Shah NM. Modular genetic control of sexually dimorphic behaviors. Cell. 2012; 148:596–607. [PubMed: 22304924]

Yang CF, Chiang MC, Gray DC, Prabhakaran M, Alvarado M, Juntti SA, Unger EK, Wells JA, Shah NM. Sexually Dimorphic Neurons in the Ventromedial Hypothalamus Govern Mating in Both Sexes and Aggression in Males. Cell. 2013; 153:896–909. [PubMed: 23663785]

Yoon H, Enquist LW, Dulac C. Olfactory inputs to hypothalamic neurons controlling reproduction and fertility. Cell. 2005; 123:669–682. [PubMed: 16290037]

Zufall F, Leinders-Zufall T. Mammalian pheromone sensing. Current Opinion in Neurobiology. 2007; 17:483–489. [PubMed: 17709238]

Article Highlights

- Distinct neuronal subtypes in the medial amygdala control distinct innate behaviors
- GABAergic neurons promote aggression and other social behavior in a scalable manner
- Glutamatergic neurons promote asocial, repetitive self-grooming
- Activation of one neuronal population inhibits the behaviors promoted by the other

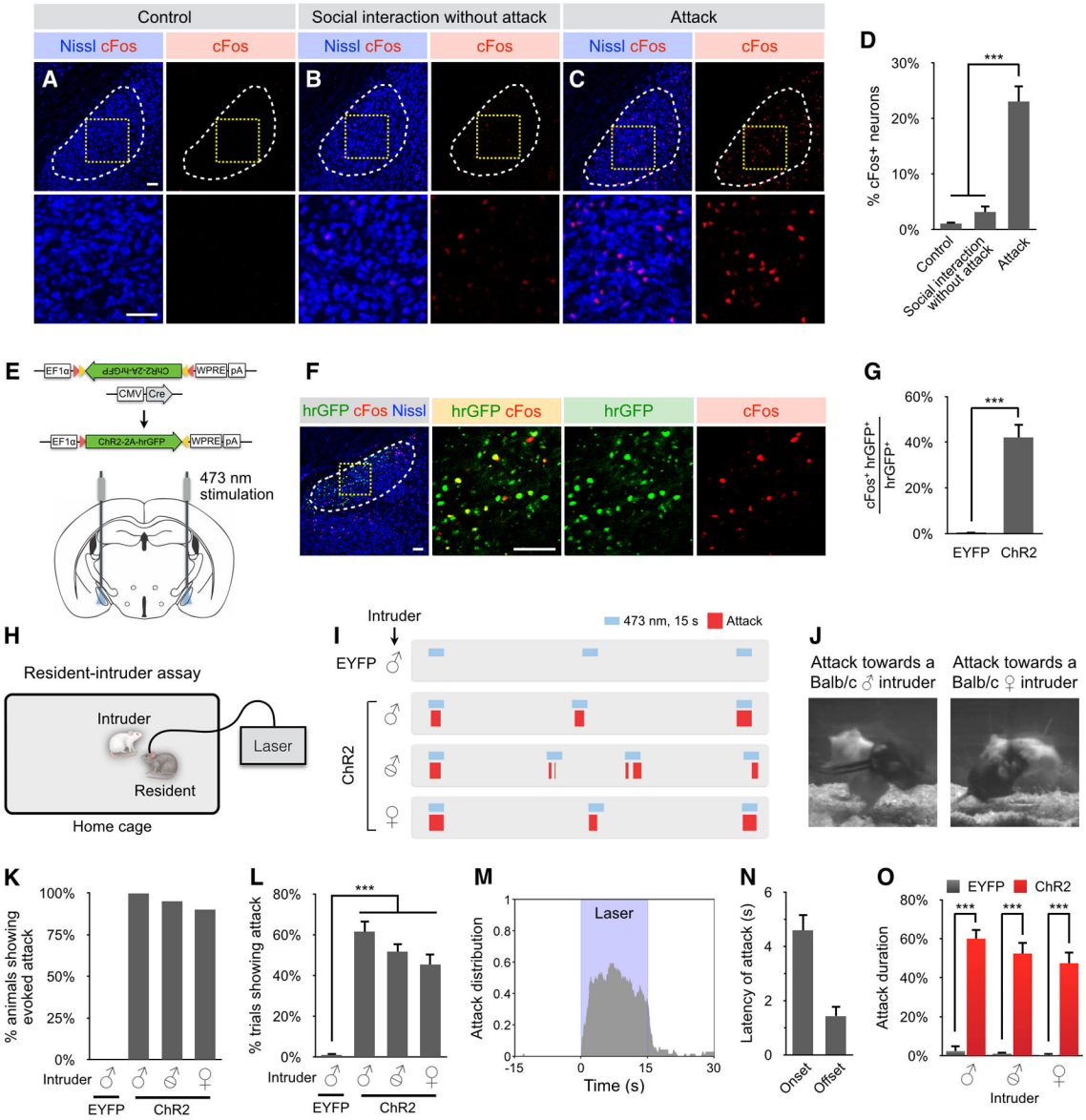

Figure 1. Functional Identification of MeApd in Aggressive Behavior

(A–D) c-fos induction in C57BL/6N resident males following offensive attack, or social interaction without attack, towards intruder males. Red, c-fos immunostaining; blue, fluorescent Nissl stain. Scale bar: 100 μm. (D) Percentage of cells expressing c-fos in each condition.

(E) Schematic illustrating ChR2 virus injection and optic fiber placement site.

(F and G) c-fos induction in EF1α::ChR2-hrGFP-expressing MeApd neurons in a solitary animal at 1 h post-illumination. Red, c-fos immunostaining; green, hrGFP native fluorescence; blue, fluorescent Nissl stain. Scale bar: 50 μm. (G) Percentage of total $hrGFP^+$ cells that express c-fos.

(H) Schematic illustrating the resident-intruder assay. See Methods and Figure S3.

(I–O) Optogenetic stimulation of MeApd triggers attack. (I) Representative raster plots illustrating attack episodes in control EYFP or ChR2-expressing males tested with BALB/c intruders (male, castrated male, female) in the resident-intruder assay. (J) Video frames taken from attack episodes. (K) Percentage of resident males that display attack. (L) Percentage of trials showing light-induced attack using laser power 1–3 mW mm^{-2}. (M) Distribution of attack episodes with respect to the initiation of laser illumination. (N) Attack onset and offset latencies (relative to initiation and termination of illumination, respectively). (O) Percentage of time spent attacking during photostimulation period. Data are mean ± SEM. ***$p < 0.001$. In (D) $n = 5$ animals for each condition. In (G), $n = 4$ animals for each condition. In (K, L), $n \geq 10$ animals for each condition. In (M) and (N), $n = 118$ trials. In (O), $n \geq 30$ trials for each condition.
See also Figures S1–S3 and Movie S1.

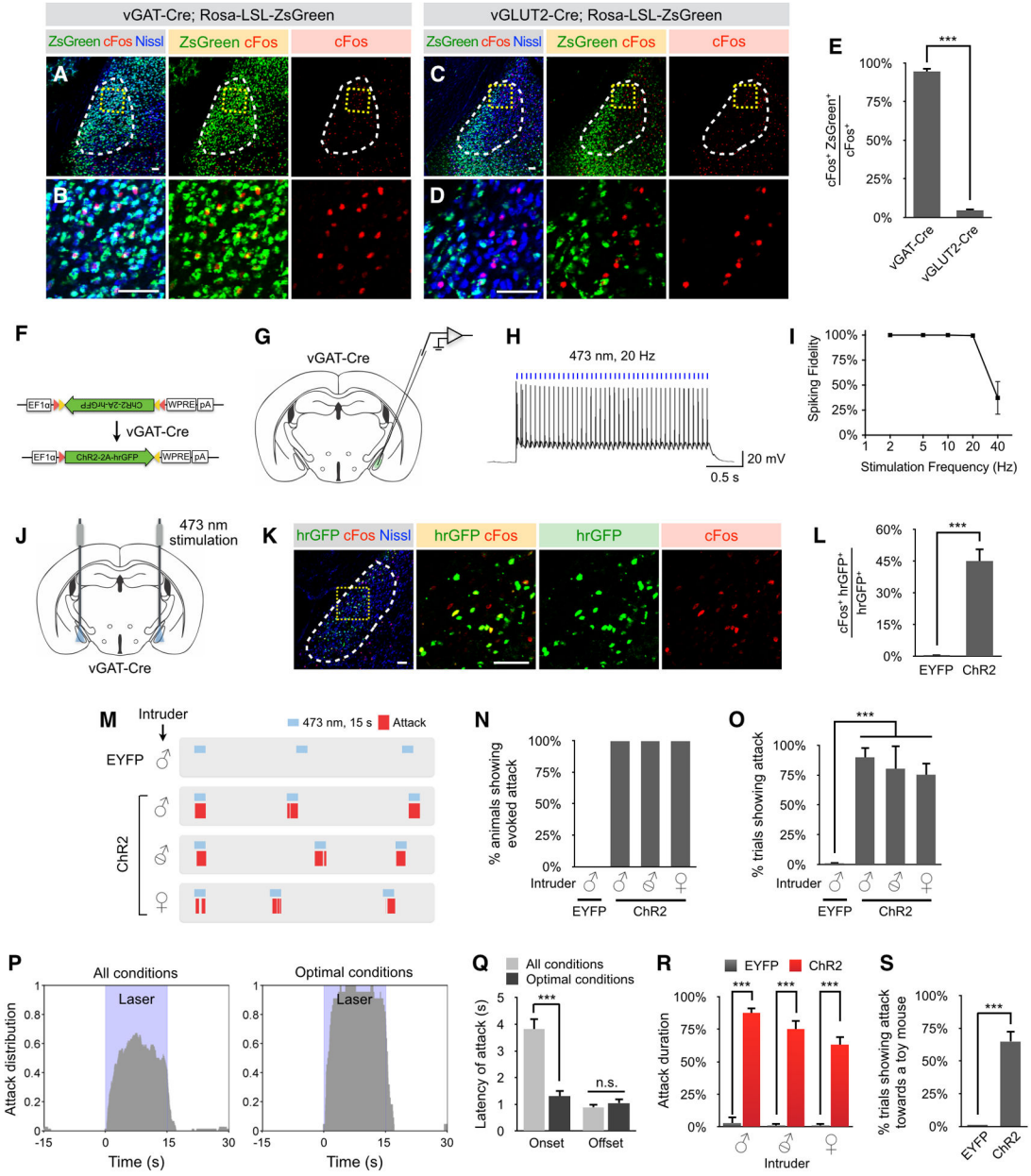

Figure 2. Optogenetic Stimulation of vGAT$^+$ Neurons in MeApd Triggers Aggressive Behavior

(A–E) vGAT$^+$ neurons in MeApd are activated during aggressive behavior. (A–D) c-fos induction in vGAT$^{Cre/+}$ or vGLUT2$^{Cre/+}$ resident males following attack towards intruder males. Resident males are double heterozygous for vGAT-Cre and Rosa-LSL-ZsGreen (Ai6), or double heterozygous for vGLUT2-Cre and Rosa-LSL-ZsGreen (Ai6). Red, c-fos immunostaining; green, ZsGreen native fluorescence; blue, fluorescent Nissl stain. Scale bar: 50 μm. (E) Percentage of ZsGreen$^+$ cells expressing c-fos.

(F) Schematic illustrating the ChR2 virus injected.

(G–I) Whole-cell patch clamp recording from $vGAT^{+}$ cells in MeApd in acute brain slices. 473 nm photostimulation-evoked spiking (H) and quantification of spike fidelity (I) are shown.

(J) Schematic illustrating the optic fiber placement in $vGAT^{Cre/+}$ animals.

(K and L) c-fos induction in EF1α::ChR2-hrGFP-expressing $vGAT^{+}$ neurons in solitary animals at 1 h post-illumination. Red, c-fos immunostaining; green, hrGFP native fluorescence; blue, fluorescent Nissl stain. Scale bar: 50 μm. (L) Percentage of $hrGFP^{+}$ cells expressing c-fos.

(M–S) Optogenetic stimulation of MeApd $vGAT^{+}$ neurons triggers attack. (M) Representative raster plots illustrating attack episodes in control or ChR2-expressing $vGAT^{Cre/+}$ males tested with BALB/c intruders (male, castrated male, female) in the resident-intruder assay. (N) Percentage of resident males that displayed attack. (O) Percentage of trials showing light-induced attack using laser power 1–3 mW mm^{-2}. (P) Distribution of attack episodes with respect to the initiation of laser illumination. Left panel, all conditions; right panel, optimal conditions (resident was facing the intruder and within half a body-length). (Q) Attack onset and offset latencies (relative to initiation and termination of illumination, respectively). (R) Percentage of time spent attacking during photostimulation period. (S) Percentage of trials showing optogenetically evoked attack towards an inanimate toy mouse.

Data are mean ± SEM. n.s.: $p > 0.05$, ***$p < 0.001$. In (E) and (L), n = 4 animals for each condition. In (I), n = 5 cells. In (N) and (O), n≥10 animals for each condition. In (P) and (Q), n = 93 trials for all conditions and n = 22 trials for optimal conditions. In (R), n≥25 trials for each condition. In (S), n = 5 animals for each condition.

See also Figures S2, S5 and Movie S2.

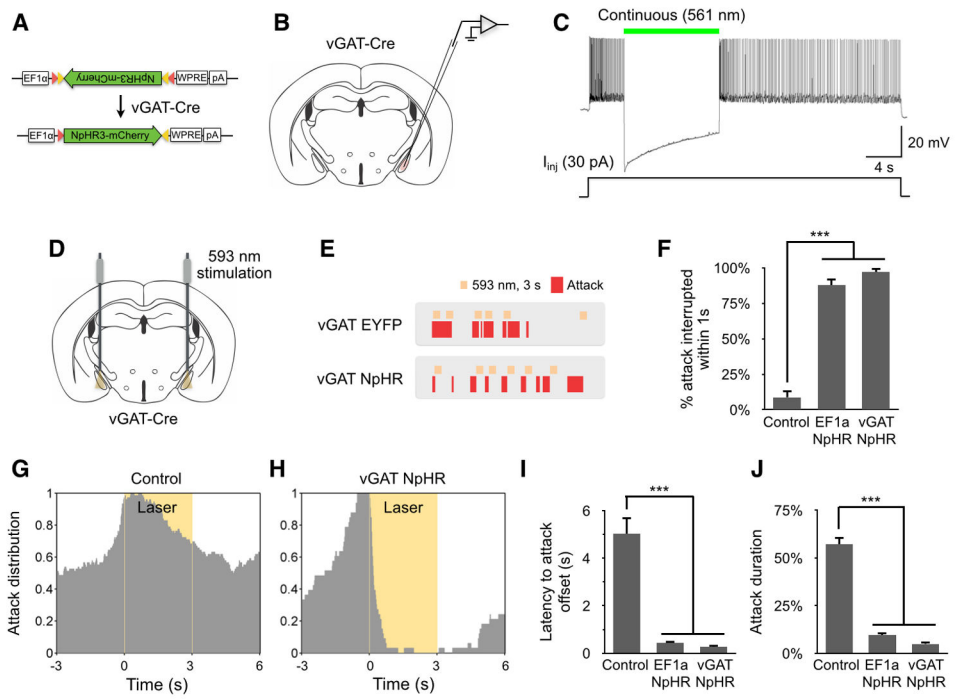

Figure 3. The Activity of MeApd vGAT^{+} Neurons Is Required for Ongoing Aggressive Behavior

(A) Schematic illustrating the Cre-dependent eNpHR3 virus injected in vGAT$^{Cre/+}$ animals.

(B–C) Whole-cell patch clamp recording in acute brain slices, showing photostimulation-induced suppression of current injection-evoked spiking in eNpHR3-mCherry expressing vGAT^{+} cells in MeApd (C).

(D) Schematic illustrating the optic fiber placement in vGAT$^{Cre/+}$ animals.

(E) Representative raster plots illustrating attack episodes in control or eNpHR3-expressing males tested with intact BALB/c male intruders in the resident-intruder assay.

(H) Percentage of attack episodes interrupted within 1 second after the initiation of the laser illumination.

(G–H) Distribution of attack episodes with respect to the initiation of laser illumination in control or eNpHR3-expressing males paired with male intruders.

(I) Latencies to interrupt attack with respect to the initiation of the laser illumination.

(J) Percentage of time spent attacking during the 3 s photostimulation period

Data are mean ± SEM. ***p < 0.001. In (F–J), n = 116 trials for control, n = 81 trials for EF1α eNpHR3, and n = 63 trials for vGAT eNpHR3.

See also Figures S2, S4 and Movie S3.

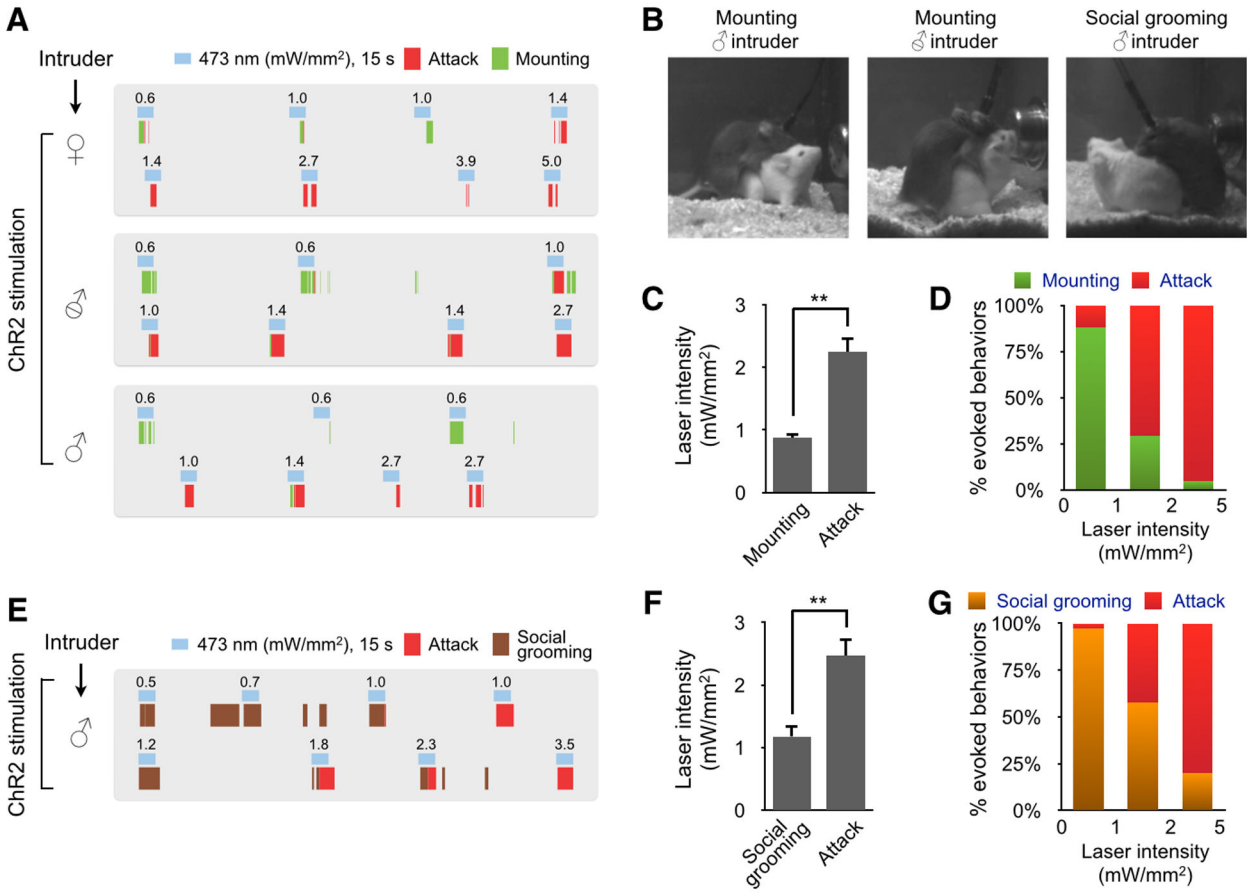

Figure 4. MeApd vGAT$^+$ Neurons Control Different Social Behaviors in a Scalable Manner

(A and E) Representative raster plots illustrating different social behavior episodes in control or ChR2-expressing males tested with BALB/c intruders (male, castrated male, female) in the resident-intruder assay. Laser pulses were delivered at different indicated illumination intensities.

(B) Video frames taken from behavioral episodes with BALB/c male (intact or castrated) intruders.

(C and F) Average laser illumination intensities that trigger different social behaviors.

(D and G) Percentage of evoked behaviors at different ranges of laser illumination intensities. Upon low intensity stimulation, we observed mounting in 8 animals and social grooming in 6 animals.

Data are mean ± SEM. **p < 0.01. In (C–D, F–G), n≥40 trials for each condition.

See also Movie S4.

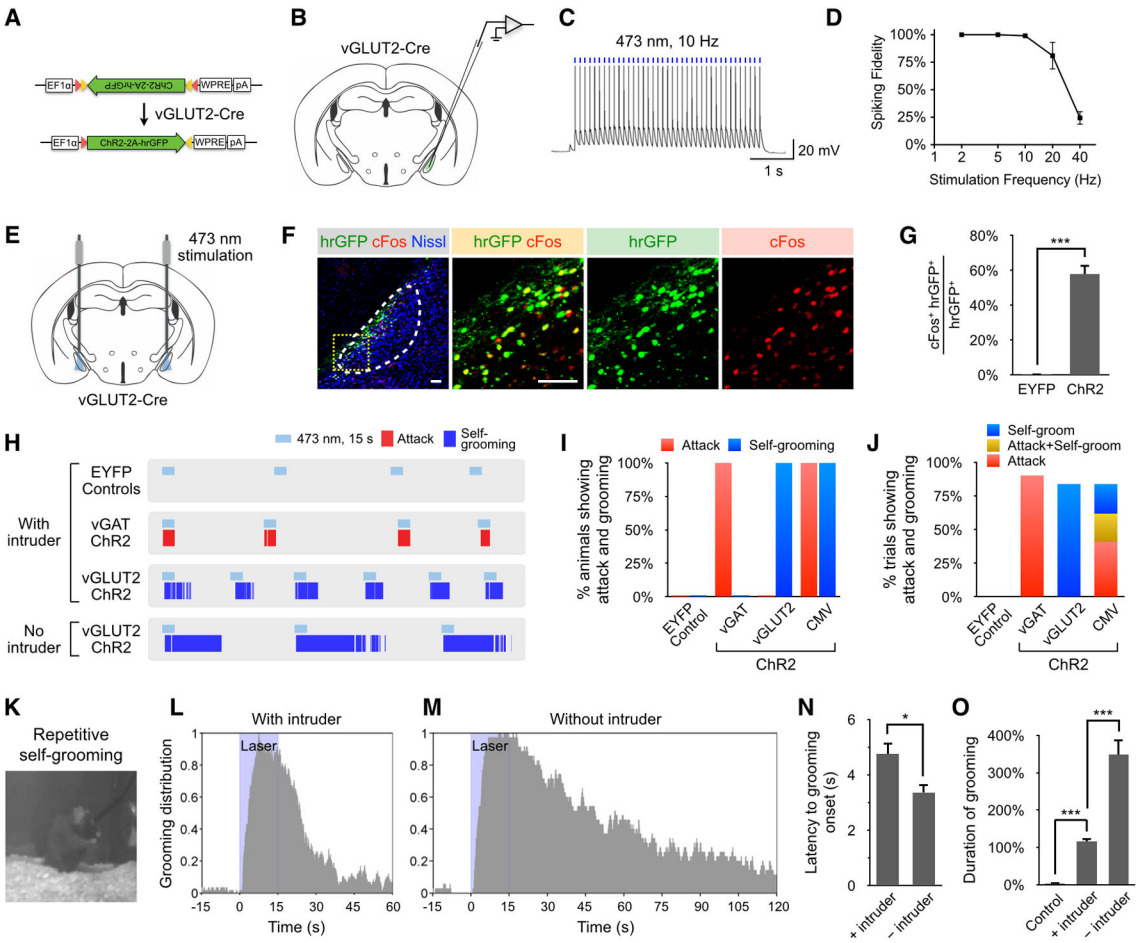

Figure 5. Neighboring vGLUT2^{+} Neurons Promote Self-grooming

(A) Schematic illustrating the ChR2 virus injected.

(B–D) Whole-cell patch clamp recording from vGLUT2^{+} cells in MeApd in acute brain slices. 473 nm photostimulation-evoked spiking (C) and quantification of spike fidelity (D) are shown.

(E) Schematic illustrating optic fiber placement in vGLUT2$^{Cre/+}$ animals.

(F and G) c-fos induction in EF1α::ChR2-hrGFP-expressing vGLUT2^{+} neurons in solitary animals at 1 h post-illumination. Red, c-fos immunostaining; green, hrGFP native fluorescence; blue, fluorescent Nissl stain. Scale bar: 50 μm. (G) Percentage of total hrGFP^{+} cells expressing c-fos.

(H) Representative raster plots illustrating self-grooming episodes in EYFP control and ChR2-expressing males in the presence or absence of intact BALB/c intruder males.

(I) Percentage of resident males showing evoked attack or self-grooming. CMV: Non-selective expression of ChR2 in MeApd by co-injecting AAVs expressing CMV-Cre and Cre-dependent ChR2.

(J) Percentage of trials showing evoked attack or self-grooming using laser power 1–3 mW mm^{-2}.

(K) Video frame taken from repetitive self-grooming episodes.

(L–M) Distribution of self-grooming episodes with respect to the initiation of laser illumination in ChR2-expressing males in the presence or absence of intruder animals.
(N) Onset latencies of self-grooming relative to the initiation of illumination.
(O) Percentage of time spent self-grooming during the 15 s photostimulation period.
Data are mean ± SEM. *$p < 0.05$, ***$p < 0.001$. In (D), n = 4 cells. In (G), n = 4 animals for each condition. In (I–J), n≥10 animals for each condition. In (L–O), n = 79 trials for ChR2 animals with intruders, n = 37 trials for ChR2 animals without intruders, and n = 25 trials for control.
See also Figures S2, S5 and Movie S5.

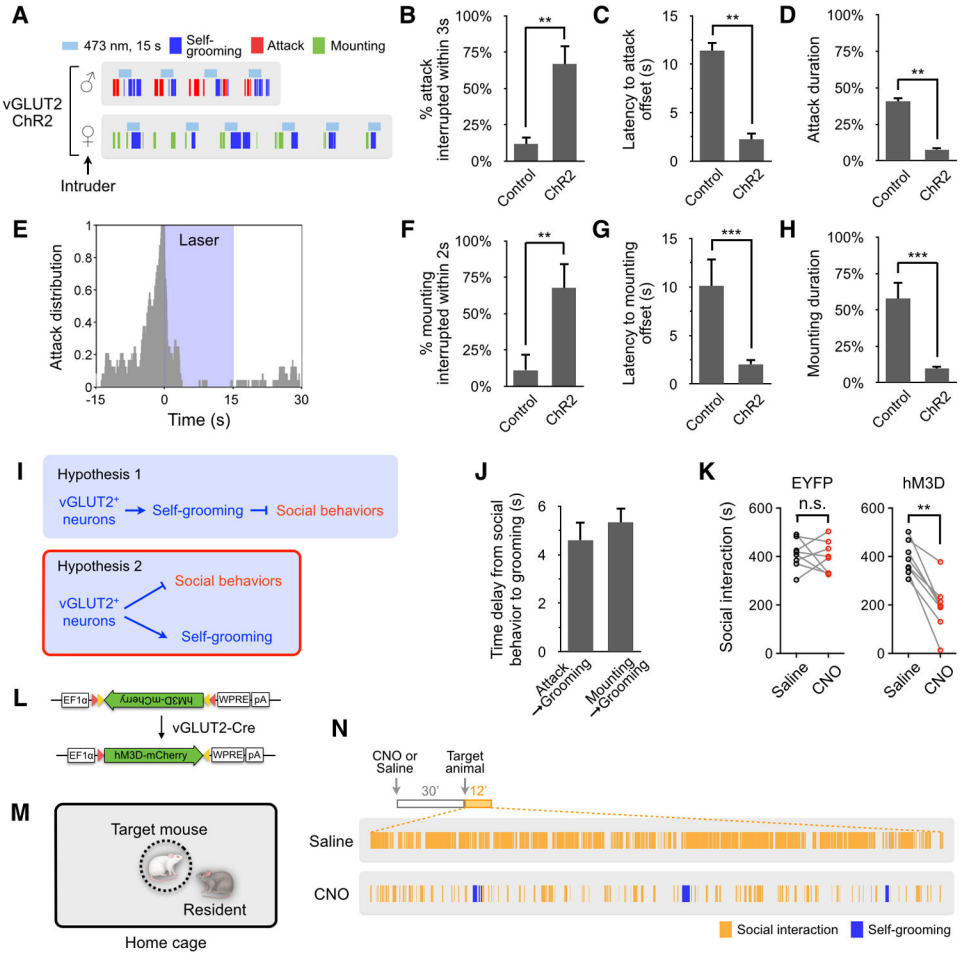

Figure 6. vGLUT2$^+$ Neurons Suppress Naturally Occurring Social Behaviors

(A–H, J) ChR2 activation of vGLUT2$^+$ neurons suppresses ongoing social behavior. (A) Representative raster plots illustrating attack, mounting and self-grooming behavior in the presence of BALB/c intruder mice. (E) Distribution of attack episodes with respect to the initiation of laser illumination in ChR2-expressing males. (B, F) Percentage of attack or mounting episodes interrupted within seconds after the initiation of the laser illumination. (C, G) Latency to stop attack or mounting with respect to the initiation of the laser illumination. (D, H) Percentage of attack or mounting during the 15 s photostimulation period. (J) Time delay when transitioning from the interruption of ongoing social behavior to the onset of self-grooming.

(I) Two alternative hypotheses of how vGLUT2$^+$ neurons suppress social behaviors. (K–N) Pharmacogenetic activation of vGLUT2$^+$ neurons reduces social interaction in a modified resident-intruder assay. (L) Schematic illustrating the Cre-dependent hM3D virus injected. (M) Illustration of modified resident intruder assay (intruder target mice are confined in an inverted pencil cup). (N) Representative raster plots illustrating social interaction and self-grooming episodes in hM3D-expressing animals following saline or CNO administration. (K) Duration of social interaction in EYFP or hM3D-expressing animals following saline or CNO administration.

Data are mean ± SEM. **p < 0.01, ***p < 0.001. In (A–E), n≥24 trials for each condition. In (F–H, J), n≥17 trials for each condition. In (K), n = 8 animals for both hM3D and EYFP control.

See also Figure S6.

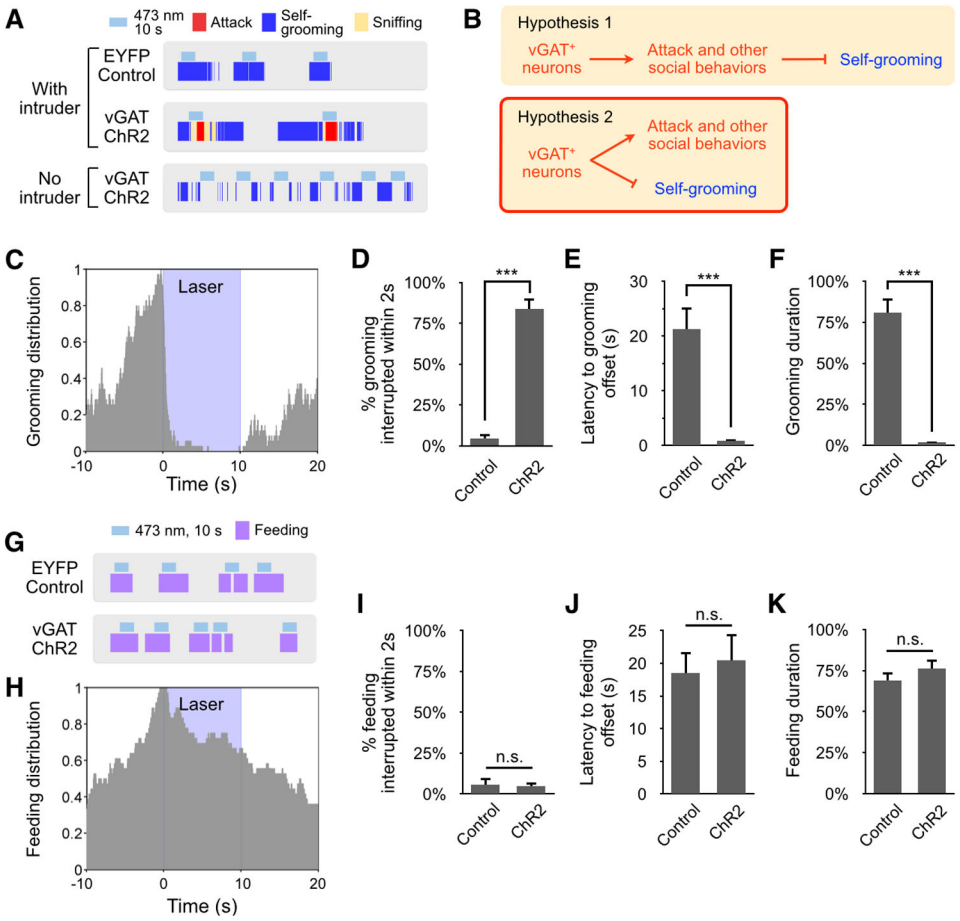

Figure 7. vGAT$^+$ Neurons Suppress Naturally Occurring Self-grooming Behavior

(A–F) ChR2 activation of vGAT$^+$ neurons in MeApd suppresses ongoing self-grooming behavior. (A) Representative raster plots illustrating sniffing, attack and self-grooming behavior episodes in the presence or absence of intact BALB/c intruder males. (B) Two alternative hypotheses of how vGAT$^+$ neurons suppress self-grooming. (C) Distribution of self-grooming episodes with respect to the initiation of laser illumination in ChR2-expressing males. (D) Percentage of self-grooming episodes interrupted within two seconds after the initiation of the laser illumination. (E) Latency to stop self-grooming with respect to the initiation of the laser illumination. (F) Percentage of time spent self-grooming during the 15 s photostimulation period. In (C–F), optogenetic stimulations are applied to solitary animals.

(G–K) ChR2 activation of vGAT$^+$ neurons in MeApd does not suppress ongoing feeding behavior. (G) Representative raster plots illustrating feeding episodes in the absence of intruders. (H) Distribution of feeding episodes with respect to the initiation of laser illumination in ChR2-expressing males. (I) Percentage of feeding episodes interrupted within two seconds after the initiation of the laser illumination. (J) Latency to stop feeding with respect to the initiation of the laser illumination. (K) Percentage of time spent feeding during the 15 s photostimulation period.

Data are mean ± SEM. n.s.: $p > 0.05$, ***$p < 0.001$. In (C–F), n = 100 trials for ChR2 experiment, n = 50 trials for control. In (H–K), n = 36 trials for each condition.
See also Figure S7 and Movie S6.